

1 Article

2 Measurement of viscoelastic properties for polymers 3 by nanoindentation

4 Yuemin Wang¹, Lei Shang¹, Panpan Zhang², Xiangqiao Yan¹, Ke Zhang³, Shuliang Dou^{1*}, Jiupeng
5 Zhao^{3*} and Yao Li^{1*}

6 ¹ Center for Composite Materials and Structures, Harbin Institute of Technology, Harbin, China

7 ² Jincheng campus, Taiyuan University of Science and Technology, Jincheng, China

8 ³ School of Chemistry and Chemical Engineering, Harbin Institute of Technology, Harbin, China

9 * Correspondence: dousl@hit.edu.cn(S.D); jpzhao@hit.edu.cn(J.Z); yaoli@hit.edu.cn(Y.L)

10 **Abstract:** A method for measuring the mechanical parameters of viscoelastic polymers by
11 nanoindentation technology was proposed and verified. Through the mechanical response of load-
12 displacement curves at different loading rates, then creep compliances and relaxation modulus were
13 fitted. Polyimide thin film was employed in this research and experiments for five different loading
14 rates were conducted. The fitting load-displacement loading curves obtained by the inversion
15 method were identical to the experimental curves at five different loading rates, confirming the
16 validity of the method. Moreover, with the loading rates increased, the fitting curves were more
17 consistent commensurately with the nanoindentation experiment. DMA experiments were tested,
18 and the generalized Kelvin/ Maxwell model were used for fitting experiment data. Results from
19 DMA tests generally agree well with data from nanoindentation method, thereby verifying the
20 feasibility of the method. The Prony series obtained by the two methods were used to simulate the
21 creep experiments, which further verified the method.

22 **Keywords:** nanoindentation; viscoelasticity; creep compliance; relaxation modulus; Prony
23 series

24

25 1. Introduction

26 With the increasing use of very small structures, nanocomposites and other micro-materials in
27 various engineering areas such as optic, mechanical, electric and micro-electromechanical systems, a
28 critical evaluation of the mechanic behavior is needed to predict the reliability of such materials [1-
29 5]. Traditional mechanical testing is not suitable for small-scale or local performance testing due to
30 the limitations of sample size, experimental conditions and test resolution [6-9]. Nanoindentation
31 technology has become one of the most important methods for small-scale measurement because of
32 its advantages of high resolution, simple sample preparation and non-destructive testing [10-14]. For
33 general materials, nanoindentation technology can easily acquired hardness and elastic modulus, and
34 more importantly, in the plastic region, the inversion calculation of constitutive relation can be
35 carried out by dimensional analysis [15-17]. However, for time-dependent materials, the viscoelastic
36 parameters cannot be directly measured, and the inversion calculation method proposed by previous
37 researchers is not suitable, so how to obtain the mechanical properties of viscoelastic materials is one
38 of the emphases. Unfortunately, there are few studies on calculation of viscoelastic parameters using
39 nanoindentation.

40 Pal Jen Wei et al. [18] proposed the combination of one dashpot in series with one Kelvin model
41 and two Kelvin models with distinct time constants in series to describe the deformation of polymers
42 under indentation tests. A coupled experimental/numerical approach for the characterization of the
43 local mechanical behavior of epoxy polymer materials was proposed by M. Minervino et al. They
44 found that the pure viscoelastic constitutive law is not able to reproduce the local polymer behavior

45 and needs be enhanced by adding material softening behavior [19]. Menčík J et al. [20] proposed a
 46 model consist of spring, plastic element, dashpot and two Kelvin–Voigt bodies to calculate the load
 47 response of viscoelastic-plastic materials, including biological and restorative biomaterials. In
 48 addition, some other models for viscoelastic polymers have been proposed as well [21-26]. Although
 49 efforts have been made to explain the viscoelastic properties of polymers, the models suggested in
 50 the previous studies are either very complex, resulting in time-consuming calculations or based on
 51 complex input data, such as complex loading profiles. On the other hand, the parameters obtained
 52 cannot be directly applied to engineering mechanical calculations, especially for simulation
 53 calculations.

54 The paper will propose and validate a method to directly calculate the viscoelastic
 55 parameters using nanoindentation test. The polyimide thin film (PI) was used to
 56 validate this method in this paper. The method can be acquiring creep compliance
 57 and relaxation modulus based on nanoindentation experiments at different loading
 58 rates. Comparatively, the DMA creep experiments were carried out, and then the
 59 viscoelastic parameter fitted by the generalized Kelvin/ Maxwell model, so that they
 60 can be used to compare with the results of nanoindentation method. Finally, Prony
 61 series calculated by the two methods are used in the creep simulation for verifying
 62 the method.

63 2. Theoretical background

64 The nanoindentation test can be regarded as a process in which a rigid indenter is gradually
 65 pressed into an elastic half-space. For a conical indenter, the relationship between load and
 66 displacement can be obtained by Sneddon contact model [27, 28].

$$P = \frac{4}{\pi(1-\nu)\tan\alpha} Gh^2 \quad (1)$$

67 Similarly, according to this line of thought, when testing viscoelastic materials, the experimental
 68 process can be regarded as a quasi-static boundary issue between rigid indenter and semi-infinite
 69 space materials with time dependence. The difference between them is that viscoelastic materials
 70 have creep or relaxation characteristics due to their time dependence properties. Therefore, how to
 71 introduce time variable into contact model is a key factor. Load-displacement curve involves time
 72 factors such as loading rate, holding time, unloading rate, etc. In this paper, loading rate was used to
 73 express time variables.

74 According to Riande's research[29], the hereditary integral operator is introduced to equation
 75 (1) leads to the relationship between displacement and load:

$$h^2(t) = \frac{\pi(1-\nu)\tan\alpha}{4} \int_0^t J(t-\xi) \left[\frac{dp(\xi)}{d\xi} \right] d\xi \quad (2)$$

76 where $J(t)$ is the creep compliance.

77 The indentation load could be shows as $P(t) = v_0 t H(t)$ by the constant loading rate, where v_0
 78 being the loading rate and $H(t)$ the Heaviside unit step function. Let substitute $P(t)$ into
 79 equation(2), we have

$$h^2(t) = \frac{\pi(1-\nu)v_0 \tan\alpha}{4} \int_0^t J(t-\xi) d\xi \quad (3)$$

80 Differentiating equation (3) with respect to t , we have

$$J(t) = \frac{8h}{\pi(1-\nu) \tan \alpha} \frac{dh}{dp} \quad (4)$$

81 The general representation of the creep compliance based on the Kelvin model is

$$J(t) = J_0 + \sum_{i=1}^N J_i (1 - e^{-t/\tau_i}) \quad (5)$$

82 where $J_0, J_1, J_2, \dots, J_n$ are compliance numbers, $\tau_1, \tau_2, \dots, \tau_n$ are retardation times, and N is a
83 positive integer.

84 Substituting equation (5) into equation (4), we have

$$h^2(t) = \frac{1}{4} \pi(1-\nu) \tan \alpha \left[(J_0 + \sum_{i=1}^N J_i) P(t) - \sum_{i=1}^N J_i v_0 \tau_i (1 - e^{-P(t)/(v_0 \tau_i)}) \right] \quad (6)$$

85 Equation (6) is the viscoelastic contact model based on nanoindentation technology. Apply the
86 nanoindentation experiments at different loading rates, the relationship between loads and
87 displacement squares can be obtained, and different creep parameters can be fitted soon. Therefore,
88 the equation can analyze the viscoelastic relationship of time-dependent materials. According to the
89 Laplace transformation, there is a conversion relationship between creep compliance and relaxation
90 modulus in the Laplace domain, as shown in the equation (7), hence the relaxation modulus can be
91 obtained by creep compliance [30].

$$E(t) = L^{-1}\{\tilde{E}(s)\} = L^{-1}\left(\frac{1}{s^2 \tilde{J}(s)}\right) \quad (7)$$

92 where $E(t)$ is relaxation modulus, $L\{\}$ is Laplace operator.

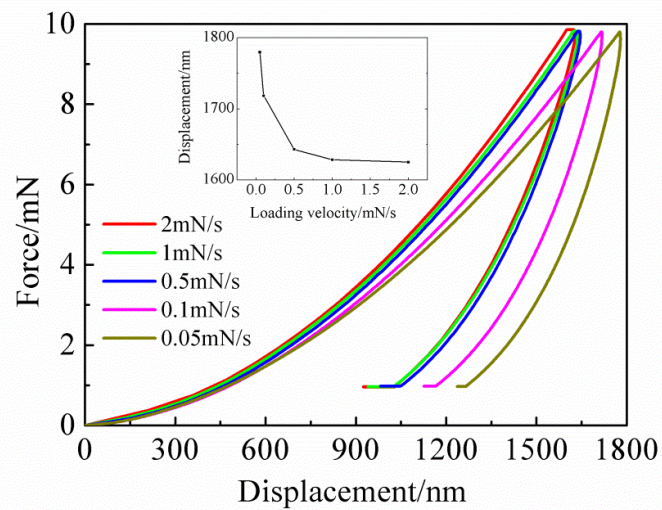
93 3. Experiments

94 A commercial polyimide thin film was adopted in our study. The polyimide precursor reacted
95 from the pyromellitic dianhydride (PMDA) and p,p'-oxy-dianiline (ODA). Specimen surface was
96 cleaned and all specimens were aged for approximately 48 hours before nanoindentation tests. All
97 nanoindentation tests were performed at room temperature. Nanoindentation experiments were
98 carried out in a stress loading manner, and the constant loading is 10 mN. Five fixed loading rates of
99 2 mN/s, 1 mN/s, 0.5 mN/s, 0.1 mN/s and 0.05 mN/s were tested, respectively. For each sample, at least
100 five tests were conducted to calculate the average value of the mechanical parameters.

101 Similarly, after the surface cleaning, samples were prepared by the mechanical cutting for DMA
102 creep tests. The creep tests of PI film were performed with film tension mode using DMA Q800 (TA
103 Instruments, DE, USA) dynamic mechanical analyzer. The DMA tests were performed under
104 controlled stress. In order to improve the accuracy of the tests, a preliminary test was carried out at
105 room temperature with the constant stress equal to 0.1MPa. Immediately after the preliminary test,
106 the samples were keeping 30 min at the test temperature. The initial stress was 5MPa. Therefore when
107 the stress reached the setting point, the value of strain with time change was recorded, and then the
108 creep curves were obtained.

109 4. Results and discussion

110 The experimental curves of nanoindentation are shown in Fig. 1. It is obvious that when the
111 maximum loads in the same value, different loading rates show the same trend of variation, however,
112 show the different maximum displacements. This indicates that polyimide film has time dependence,
113 so when the time for reaching the maximum load is different, causing different curve values.



114

115

116

Figure 1. The load-displacement curves for PI materials by nanoindentation under different loading rates.

117

118

119

120

121

122

123

124

It is noteworthy that when the loading rate is larger, the load-displacement curves obtained by the experiment basically coincide with each other. With the decrease of loading rate, the discrete phenomenon of load-displacement curve begins to appear. The slower the loading rate, the more obvious the discrete phenomenon of displacement curves. This is because the polyimide thin film is viscoelastic material, which is time-dependent. When the loading rate is slower, thus the loading time is longer. Therefore, creep phenomenon occurs during the loading process, which is consistent with the research in other literature [31-33].

125

126

127

128

According to the nanoindentation test data and the equation (5), the relationship between $h^2(t)$ and $P(t)$ under different loading rates can be obtained, the creep compliance can be analyzed.

Owing to the angle between the indenter and the measured material plane is 19.7° , the equation (6) can be simplified as follows

$$h^2(t) = 0.1883 \left[(J_0 + \sum_{i=1}^N J_i) P(t) - \sum_{i=1}^N J_i v_0 \tau_i (1 - e^{-P(t)/(v_0 \tau_i)}) \right] \quad (8)$$

129

The data of load-displacement curves at five loading rates are introduced and we

130

get

131

when the loading rate is 2 mN/s,

$$h^2(t) = 0.1883 \left[0.0012953 P(t) - 0.00319 (1 - e^{-P(t)/18.46}) - 0.0054 (1 - e^{-P(t)/172.42}) - 0.3068 (1 - e^{-P(t)/2000}) \right] \quad (9)$$

132

when the loading rate is 1 mN/s,

$$h^2(t) = 0.1883 \left[0.0012953 P(t) - 0.001596 (1 - e^{-P(t)/9.32}) - 0.0027 (1 - e^{-P(t)/86.21}) - 0.1534 (1 - e^{-P(t)/1000}) \right] \quad (10)$$

133

when the loading rate is 0.5 mN/s,

$$h^2(t) = 0.1883[0.0012953P(t) - 0.000798(1 - e^{-P(t)/4.66}) - 0.00135(1 - e^{-P(t)/43.105}) - 0.0766(1 - e^{-P(t)/500})] \quad (11)$$

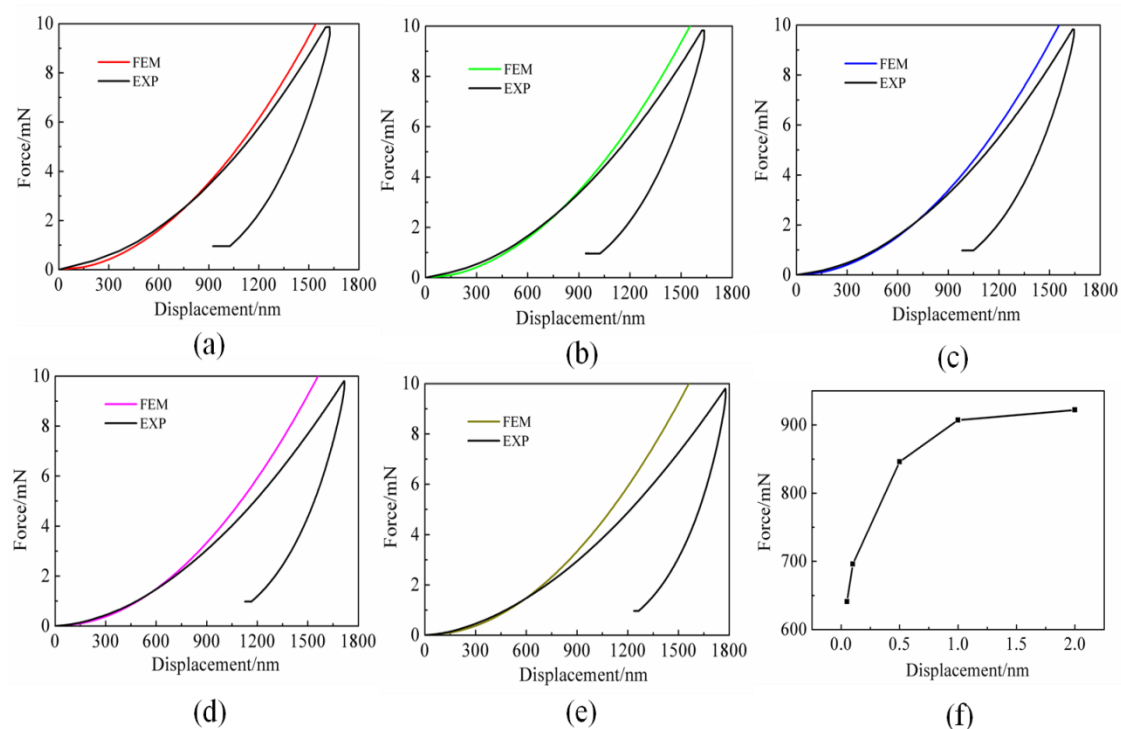
134 when the loading rate is 0.1 mN/s,

$$h^2(t) = 0.1883[0.0012953P(t) - 0.0001596(1 - e^{-P(t)/0.932}) - 0.00027(1 - e^{-P(t)/8.621}) - 0.01532(1 - e^{-P(t)/100})] \quad (12)$$

135 when the loading rate is 0.05 mN/s,

$$h^2(t) = 0.1883[0.0012953P(t) - 0.0000798(1 - e^{-P(t)/0.466}) - 0.000135(1 - e^{-P(t)/4.315}) - 0.00766(1 - e^{-P(t)/50})] \quad (13)$$

136 The fitted loading curve can be inverted by the equations (9)-(13), and then compared with the
 137 loading curve of nanoindentation experiment, as shown in Fig. 2. It can be seen that the loading curve
 138 under five different loading rates calculated by viscoelastic contact model of nanoindentation is
 139 consistent with the nanoindentation experiment, and the value dispersion is smaller, especially in the
 140 case of shallow indentation depth. It can also be seen that with the increase of the loading depth, the
 141 fitting curve and the experimental curve have certain discrete deviation. However, the overall fitting
 142 degree is good, which verifies the validity of the function based on nanoindentation technology. It
 143 can be seen that with the increase of loading rate, the position of discrete points in the loading curve
 144 is larger, which fully demonstrates the viscoelastic behavior of polyimide film. At the same time, it
 145 also shows that the function proposed in this paper is applicable to the shallow loading depth
 146 experiments, and with the increase of indentation depth, the error gradually appears.



147

148

149

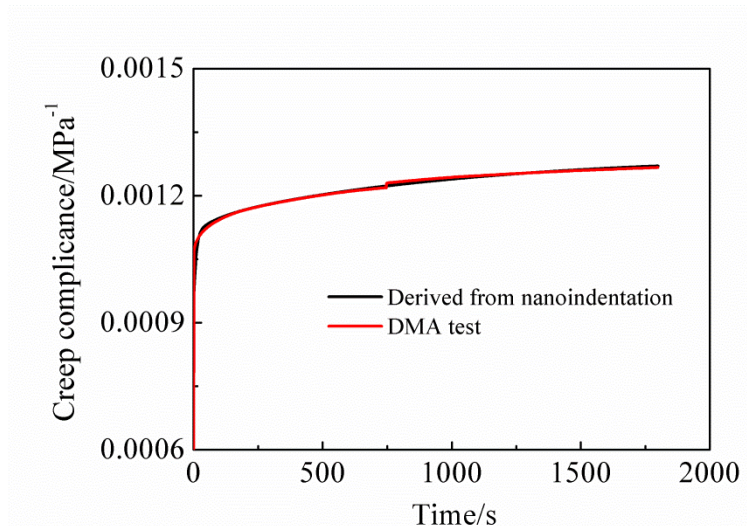
Figure 2. Fitting curves and discrete points at different loading rates. (a)2mN/s, (b)1mN/s
 ,(c)0.5mN/s, (d)0.1mN/s ,(e)0.05mN/s, (f) discrete points at different loading rates

150

According to equations (9)-(13), creep compliance of polyimide film can be deduced

$$J(t) = 0.0009397 + 0.0001712(1 - e^{-t/9.23}) + 0.00003104(1 - e^{-t/86.21}) + 0.0001534(1 - e^{-t/1000}) \quad (14)$$

151 Fig.3 is the creep compliance curves comparison obtained between the inversion of viscoelastic
 152 contact model based on nanoindentation technology and DMA creep experiments. It can be
 153 concluded that the two curves have the same development trend, less discrete in creep compliance
 154 values and in good fitting degree with the increase of time. These proved that the viscoelastic contact
 155 model based on nanoindentation technology is reasonable, and the creep compliance calculation
 156 method based on nanoindentation experiment is feasible.



157

158 **Figure 3.** Creep compliance comparisons between derived from nanoindentation experiment and
 159 DMA test.

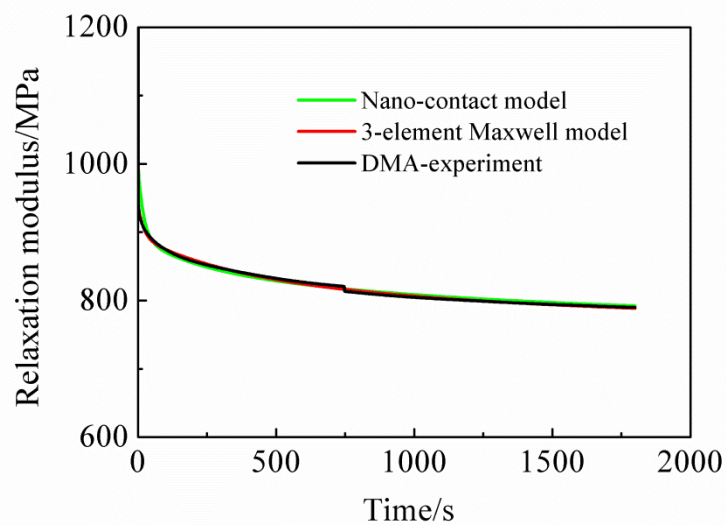
160 According to the equation (7), the calculated creep compliance can be converted into relaxation
 161 modulus, and it can be concluded that:

$$E(t) = 775 + 104.4e^{-t/20} + 40.85e^{-t/200} + 76.44e^{-t/1200} \quad (15)$$

162 Similarly, the creep compliance calculated by DMA experiment can transformed for relaxation
 163 modulus. By introducing the parameters into the 3-element generalized Maxwell model (Supporting
 164 Information), the equation can be obtained:

$$E(t) = 771.4 + 45.93e^{-t/20} + 45.58e^{-t/300} + 76.67e^{-t/1200} \quad (16)$$

165 Fig.4 is the comparison of relaxation modulus between the transformed of DMA creep
 166 experiment, fitted by 3-element Maxwell model and calculated by viscoelastic contact model based
 167 on nanoindentation. It can be concluded that the three types of data have good fitting degree, which
 168 indicates that the results from the viscoelastic contact model is consistent with those from the
 169 traditional viscoelastic model, and verified the method.



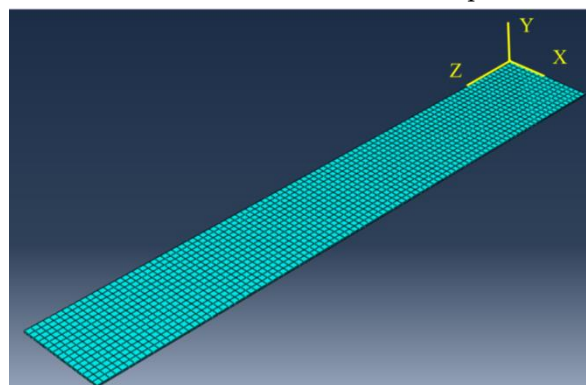
170

171 **Figure 4.** The curves of relaxation modulus by the method of 3-element Maxwell model, viscoelastic
 172 contact model based on nanoindentation and transformed of DMA creep experiment.

173 To be concluded, the viscoelastic model based on nanoindentation technology can calculate both
 174 the relaxation modulus and creep compliance. The calculated results are basically consistent with the
 175 traditional experiments, so it provided a new method to acquire viscoelastic properties.

176 5. FEM simulation

177 In order to further verify the viscoelastic parameters obtained by nanoindentation, the FEM is
 178 used to simulate creep test. The same size as the DMA test sample is selected to establish the
 179 geometric model, as shown in Fig.5. In this model, three-dimensional C3D8R element and hexahedral
 180 mesh are used. One end of the finite element geometric model is fully constrained and the opposite
 181 side is imposed with initial stress without constraint for other aspects.



182

183

Figure 5. The simulation geometric model of PI thin film.

184 The simulation is carried out in two steps. The first step is quasi-static loading with the purpose
 185 to exert the initial stress; the second step is viscous loading, keeping the initial stress for 30 min, and
 186 observing the occurrence of creep phenomena in this time range. The parameters input to the model
 187 are Prony series converted by the creep compliance, as shown in Table 1.

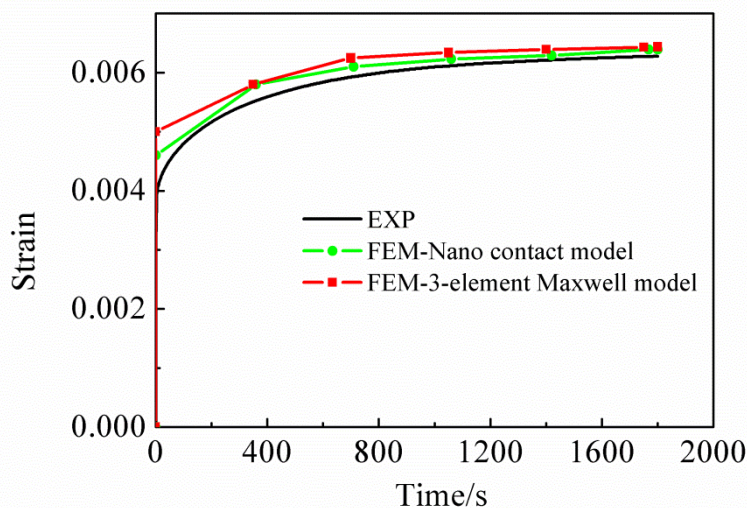
188

Table 1. Prony series under two methods.

Prony series	DMA test	Nanoindentation
$G_i=K_i$	0.0489	0.1047

$G_2=K_2$	0.0485	0.0410
$G_3=K_3$	0.0816	0.0767

189 Fig.6 is the comparison of the creep results between the input two types of Prony series and
 190 experiment. It can be seen that the simulation curves obtained by the two methods are well consistent
 191 with the experimental curves of DMA. The experimental data curves are slightly lower than the
 192 simulated data curves, but the overall error is small, which verifies the accuracy of the method. It is
 193 proved that the viscoelastic model based on nanoindentation can be applied to polyimide materials,
 194 and it also provides a calculation method for other viscoelastic polymers.



195

196 **Figure 6.** The comparison of simulation results under three types of viscoelastic parameter.

197 6. Conclusion

198 A contact model for measuring viscoelastic parameters based on nanoindentation was proposed
 199 and validated. The viscoelastic mechanical response of load-displacement curve was achieved by
 200 nanoindentation experiments at different loading rates. The fitted viscoelastic parameters of the
 201 polyimide film were identical to the values fitted by traditional DMA experiments, confirming the
 202 rationality of the method. The fitting loading curves at five different rates were obtained by the
 203 inversion method, which were nearly the same as the loading curves of nanoindentation experiments.
 204 Moreover, the fitting curves were more consistent with the bigger loading rates. Based on the Prony
 205 series of the generalized Kelvin model, the finite element numerical simulation was conducted,
 206 further confirming the feasibility of this method and providing a new idea for viscoelastic polymer
 207 materials which in small scale.

208 Reference

- 209 [1] Díez-Pascual A M, Gómez-Fatou M A, Ania F, et al. Nanoindentation in polymer nanocomposites[J].
 210 Progress in Materials Science, 2015, 67: 1-94.
- 211 [2] Gibson R F. A review of recent research on nanoindentation of polymer composites and their constituents
 212 [J]. Composites Science and Technology, 2014, 105: 51-65.
- 213 [3] Voyiadjis G Z, Malekmtie L, Samadi-Dooki A. Indentation size effect in amorphous polymers based on
 214 shear transformation mediated plasticity [J]. Polymer, 2018, 137: 72-81.
- 215 [4] Yoo B G, Choi I C, Kim Y J, et al. Room-temperature anelasticity and viscoplasticity of Cu–Zr bulk metallic
 216 glasses evaluated using nanoindentation[J]. Materials Science and Engineering: A, 2013, 577: 101-104.
- 217 [5] Voyiadjis G Z, Malekmtie L. Variation of the strain rate during CSM nanoindentation of glassy polymers

- 218 and its implication on indentation size effect [J]. *Journal of Polymer Science Part B: Polymer Physics*, 2016,
219 54(21): 2179-2187.
- 220 [6] He W, Goudeau P, Le Bourhis E, et al. Study on Young's modulus of thin films on Kapton by microtensile
221 testing combined with dual DIC system [J]. *Surface and Coatings Technology*, 2016, 308: 273-279.
- 222 [7] Giró-Paloma J, Roa J J, Díez-Pascual A M, et al. Depth-sensing indentation applied to polymers: A
223 comparison between standard methods of analysis in relation to the nature of the materials[J]. *European*
224 *Polymer Journal*, 2013, 49(12): 4047-4053.
- 225 [8] Martínez R, Xu L R. Comparison of the Young's moduli of polymers measured from nanoindentation and
226 bending experiments [J]. *MRS Communications*, 2014, 4(3): 89-93.
- 227 [9] Tvergaard V, Needleman A. Polymer indentation: numerical analysis and comparison with a spherical
228 cavity model [J]. *Journal of the Mechanics and Physics of Solids*, 2011, 59(9): 1669-1684.
- 229 [10] Jin C, Ebenstein D M. Nanoindentation of compliant materials using Berkovich tips and flat tips [J]. *Journal*
230 *of materials research*, 2017, 32(2): 435-450.
- 231 [11] Yang Y. Sensitivity of nanoindentation strain rate in poly (ester-ester-ketone) using atomic force microscopy
232 [J]. *Polymer Testing*, 2016, 53: 85-88.
- 233 [12] Jin T, Niu X, Xiao G, et al. Effects of experimental variables on PMMA nano-indentation measurements [J].
234 *Polymer Testing*, 2015, 41: 1-6.
- 235 [13] Feng G, Ngan A H W. Effects of creep and thermal drift on modulus measurement using depth-sensing
236 indentation [J]. *Journal of materials research*, 2002, 17(3): 660-668.
- 237 [14] Frontini P, Lotfian S, Monclús M A, et al. High temperature nanoindentation response of RTM6 epoxy resin
238 at different strain rates [J]. *Experimental Mechanics*, 2015, 55(5): 851-862.
- 239 [15] Oliver W C, Pharr G M. An improved technique for determining hardness and elastic modulus using load
240 and displacement sensing indentation experiments [J]. *Journal of materials research*, 1992, 7(6): 1564-1583.
- 241 [16] Chollacoop N, Dao M, Suresh S. Depth-sensing instrumented indentation with dual sharp indenters [J].
242 *Acta materialia*, 2003, 51(13): 3713-3729.
- 243 [17] Dao M, Chollacoop N, Van Vliet K J, et al. Computational modeling of the forward and reverse problems
244 in instrumented sharp indentation [J]. *Acta materialia*, 2001, 49(19): 3899-3918.
- 245 [18] Wei P J, Shen W X, Lin J F. Analysis and modeling for time-dependent behavior of polymers exhibited in
246 nanoindentation tests[J]. *Journal of Non-Crystalline Solids*, 2008, 354(33): 3911-3918.
- 247 [19] Minervino M, Gigliotti M, Lafarie-Frenot M C, et al. A coupled experimental/numerical approach for the
248 modelling of the local mechanical behaviour of epoxy polymer materials [J]. *Journal of the Mechanics and*
249 *Physics of Solids*, 2014, 67: 129-151.
- 250 [20] Menčík J, He L H, Swain M V. Determination of viscoelastic-plastic material parameters of biomaterials by
251 instrumented indentation [J]. *Journal of the mechanical behavior of biomedical materials*, 2009, 2(4): 318-
252 325.
- 253 [21] Seltzer R, Mai Y W. Depth sensing indentation of linear viscoelastic-plastic solids: a simple method to
254 determine creep compliance [J]. *Engineering Fracture Mechanics*, 2008, 75(17): 4852-4862.
- 255 [22] Song R, Muliana A H, Palazotto A. An empirical approach to evaluate creep responses in polymers and
256 polymeric composites and determination of design stresses [J]. *Composite Structures*, 2016, 148: 207-223.
- 257 [23] Zhai M, McKenna G B. Viscoelastic modeling of nanoindentation experiments: A multicurve method [J].
258 *Journal of Polymer Science Part B: Polymer Physics*, 2014, 52(9): 633-639.
- 259 [24] Herbert E G, Phani P S, Johanns K E. Nanoindentation of viscoelastic solids: A critical assessment of
260 experimental methods [J]. *Current opinion in solid state and materials science*, 2015, 19(6): 334-339.

- 261 [25] Oliveira G L, Costa C A, Teixeira S C S, et al. The use of nano-and micro-instrumented indentation tests to
262 evaluate viscoelastic behavior of poly (vinylidene fluoride)(PVDF)[J]. *Polymer Testing*, 2014, 34: 10-16.
- 263 [26] Xia W, Song J, Hsu D D, et al. Understanding the interfacial mechanical response of nanoscale polymer thin
264 films via nanoindentation[J]. *Macromolecules*, 2016, 49(10): 3810-3817.
- 265 [27] Sneddon I N. The relation between load and penetration in the axisymmetric Boussinesq problem for a
266 punch of arbitrary profile [J]. *International journal of engineering science*, 1965, 3(1): 47-57.
- 267 [28] Cheng Y T, Cheng C M. General relationship between contact stiffness, contact depth, and mechanical
268 properties for indentation in linear viscoelastic solids using axisymmetric indenters of arbitrary profiles [J].
269 *Applied Physics Letters*, 2005, 87(11): 111914.
- 270 [29] Riande E, Diaz-Calleja R, Prolongo M, et al. *Polymer viscoelasticity: stress and strain in practice*[M]. CRC
271 Press, 1999.
- 272 [30] Hernandez-Jimenez A, Hernandez-Santiago J, Macias-Garcia A, et al. Relaxation modulus in PMMA and
273 PTFE fitting by fractional Maxwell model [J]. *Polymer Testing*, 2002, 21(3): 325-331.
- 274 [31] Lee Y J, Huang J M, Kuo S W, et al. Low-dielectric, nanoporous polyimide films prepared from PEO-POSS
275 nanoparticles[J]. *Polymer*, 2005, 46(23): 10056-10065.
- 276 [32] Crochon T, Li C, Lévesque M. On time-temperature-dependent viscoelastic behavior of an amorphous
277 polyimide [J]. *Mechanics of Time-Dependent Materials*, 2015, 19(3): 305-324.
- 278 [33] Xia R, Zhou H, Wu R, et al. Nanoindentation investigation of temperature effects on the mechanical
279 properties of nafion® 117[J]. *Polymers*, 2016, 8(9): 344.